Research Article

SAR Antenna Pattern Measurement by Internal Calibration Method for GF-3 Satellite

Jian Mi [ID]**, Hongbing Sun, Ying Xing, Xuhao Zhao, and Jianxin Li**

Nanjing Research Institute of Electronics Technology, Nanjing 210039, China

Correspondence should be addressed to Jian Mi; mijian@pku.edu.cn

GF-3 is the first C-band multipolarization synthetic aperture radar (SAR) satellite in China. The SAR system is equipped with an active phased array antenna to electronically generate various antenna beams. The accuracy of SAR antenna patterns is of main importance for precise SAR image processing. The traditional method for antenna pattern measurement is the near-field method but it is unable to satisfy the demand for fast measuring in-orbit. In order to measure the SAR antenna pattern quickly with high accuracy, we propose the internal calibration method. The internal calibration uses calibration signals which are routed along the nominal signal path in SAR systems, thus monitoring the gain and phase variations for each T/R channel is possible. This paper will focus on this method, including its principle, operation steps, and results, compared to the near-field method. The internal calibration method provides a valuable solution for SAR antenna pattern measurement.

1. Introduction

GF-3 satellite was successfully launched on August 10, 2016. Two follow-on satellites GF-3B and GF-3C were launched in 2021 and 2022, respectively in order to establish a radar constellation. It is the first C-band multipolarization SAR remote sensing satellite in China [1–4]. By employing the multipolarized active phased array antenna, the SAR payload can achieve the specifications of the 1-m resolution, large swath width, 12 observing modes, and 8-year-long life. The phased array antenna has the characteristics of high efficiency, high polarization isolation, high beam-steering accuracy, lightweight, high reliability, and long operating life. The performance of the antenna is much better with respect to previous similar SAR antennas, providing strong technical support for monitoring land and sea in all weather conditions regardless of day or night.

The accuracy of SAR antenna patterns is of main importance for precise SAR image processing [5, 6]. Early SAR systems with a low number of antenna beams use in-orbit antenna pattern measurements for correction, which need many ground receivers and transmitters. To meet the multiuser requirements, 12 observing modes are designed for GF-3 such as Quad-pol stripmap mode, Spotlight Mode, Wide scanSAR Mode, and Wave mode [2, 3], thus in-orbit antenna pattern measurements are uneconomical. It calls for a new method to get the antenna pattern with high accuracy and high efficiency.

The traditional method for antenna pattern measurement is the near-field method. The antenna is placed in a microwave darkroom, and a scanning frame system is used to sample the near-field of the antenna, thus the far-field pattern is calculated based on planar wave expansion theory. The near-field method has high accuracy but puts forward high requirements for test sites. For the GF-3 SAR antenna [3, 4], the aperture size is 15 m × 1.232 m, which calls for a large darkroom and a scanning frame longer than 18 m. Other requirements for the darkroom include working bandwidth, cross-polarization, shielding, EMC, and the performance of absorbing materials. Besides, a single test time for a near-field measurement is 5 hours long (8 beams at the same time) and more than 500 beams are designed for 12 working modes, so near-field method will cost a lot of time.

What is more, the near-field method can only be carried out in the ground test. When the satellite is in

TABLE 1: SAR antenna parameters of GF-3.

Parameters	Values
Central frequency	5.4 GHz
Maximum bandwidth	300 MHz
Polarization	Linear pol, dual pol, quad pol
Polarization isolation	>35 dB
T/R module power	20 W
Number of T/R modules	24(Azimuth) × 32(Elevation) for each polarization
Beamwidth	0.188°(Azimuth), 2.29°(Elevation)
Digital beam control	TX: Phase only (6 bit); RX: Amplitude (6 bit) and phase (6 bit)
Aperture size	15 m × 1.232 m
Number of panels	4
Weight	980 kg (radiating panels only)

orbit, the working state and environment are different from the ground test, especially the temperature field variation of the SAR antenna panel, leading to the antenna pattern difference. Phased array antenna calibration is applied to sample each antenna element in the array to identify the differences among the elements [7]. The calibration methods are divided into four categories: the near-filed scanning probe method, the peripheral fixed probe method, the mutual coupling method, and the built-in network method. For in-orbit calibration, the first two methods are not applicable because a probe is required. The mutual coupling method has low accuracy which is derived from the unwanted edge effects. The built-in network method, which is called the internal calibration method in the SAR system, is mostly used with high accuracy and efficiency.

In order to overcome the disadvantages of the near-field method in antenna pattern measurement, we propose the internal calibration method, which can be applied in both ground tests and in-orbit tests. In this paper, we will introduce the principle and operation steps of the internal calibration method and compare the measured antenna pattern with the near-field method. The results indicate that the internal calibration method is of high precision and high efficiency and can be expanded to in-orbit SAR antenna pattern measurement.

2. Overview

Table 1 provides a brief overview of GF-3 SAR antenna key parameters [2][3]4]. There is a significant improvement in bandwidth, output power, and polarization isolation compared to RADARSAT-II [8].

The architecture of the GF-3 SAR antenna system is shown in Figure 1. The antenna is divided into 4 panels, which consist of 6 tiles along the azimuth direction. There are 24 tiles for the antenna. Each tile is equipped with slotted waveguide antennas, 4-channel T/R modules, time delay modules (TDU), power supply module, beam control module, RF power dividers, frame, and thermal control module. The SAR antenna consists of two independent RF chains to realize H and V polarized signals and further achieve single polarization, dual-polarization, and quad-polarization modes. The two RF chains are the same.

In transmit state, the linear frequency modulated RF signal is generated by the SAR electronics subsystem and amplified by the preamplifier. Then the signal is distributed among panels and tiles through 2 : 2 and 1 : 6 power dividers. In each tile, the signal transmits to the time delay module to compensate for beam pointing dispersion after 1 : 4 power divider, further the signal is amplified to high power in the T/R module and radiates through the waveguide antenna. In the receive state, the signal flows in opposite direction. The echo signal is received by the waveguide antenna and amplified with low noise in the T/R module and time delay module and then is summed by the power dividing network. The received signal transmits to the SAR electronics subsystem to realize quantization, data compression, and data formatting. The internal calibration is realized by placing a coupler in a T/R channel and combining the coupled signal of all T/R channels.

3. Methods

3.1. Principle. For active phased array antennas, the radiated pattern F is calculated by [9]

$$F(u, v) = \sum_{m=1}^{M} \sum_{n=1}^{N} f_{mn}(u, v) \cdot a_{mn} \cdot \exp\left[jk\left(x_m u + y_n v\right)\right].$$

(1)

In this antenna model, M and N are the numbers of antenna subarrays in each dimension, $f_{mn}(u,v)$ is the pattern of antenna subarray, a_{mn} is the complex excitation coefficient of the T/R channel, x_m and y_n are the positions of antenna subarrays, and k is the wavenumber.

To get the far-field pattern of GF-3 with high accuracy, $f_{mn}(u,v)$ and a_{mn} should be measured. The pattern of each subarray is constant and can be obtained in the ground test stage. a_{mn} will change when the temperature of the T/R channel varies. The internal calibration method is applied to get the excitation coefficient of each T/R channel in real-time, both in the ground test and in-orbit test.

3.2. Internal Calibration Basics. The internal calibration uses calibration signals, which are routed as closely as possible along the nominal signal path. The calibration network is realized by placing a coupler in each T/R channel and
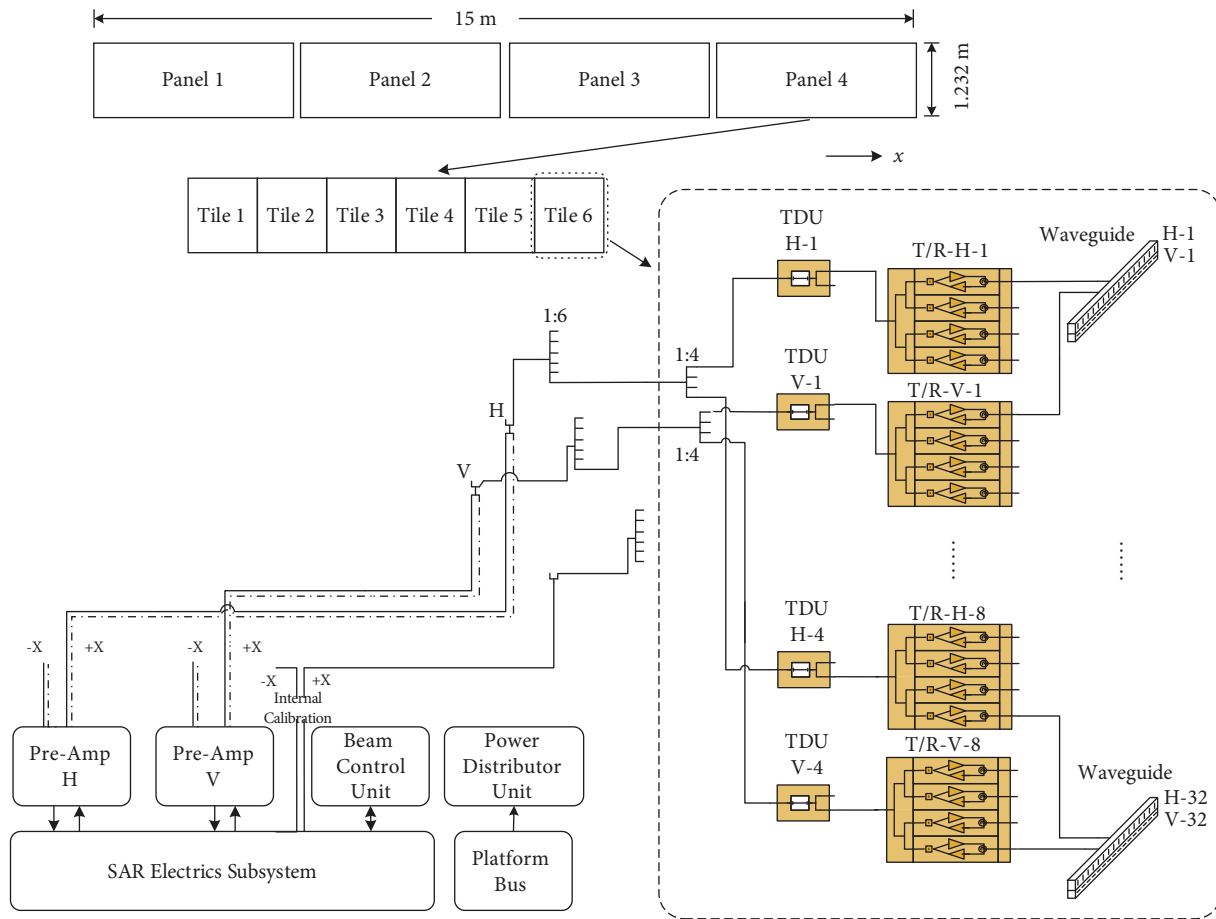
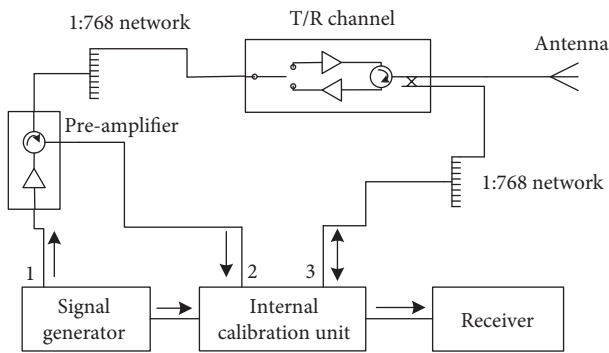FIGURE 1: The architecture of the GF-3 SAR antenna system.

FIGURE 2: Schematic diagram of the internal calibration system.

FIGURE 3: Schematic diagram of the directional coupler in the T/R channel.

combining the coupling signal of all T/R channels. The calibration signals experience the same gain and phase variations as the nominal signals. It is carried out in the SAR payload by forming transmit-receive closed RF loops [10–14]. The schematic diagram is displayed in Figure 2. RF loops are formed and switched by controlling the state of the internal calibration unit (ICU). The calibrations for both transmit and receive are similar, the differences lie in the direction of the signal.

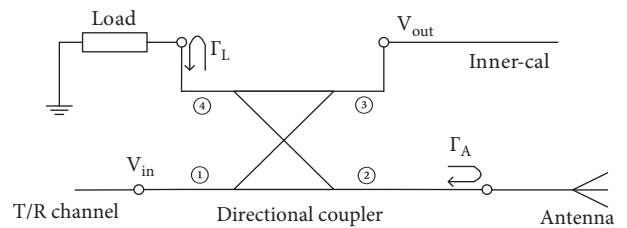For antenna pattern measurement, only one T/R channel is working at the same time. In transmit state, the RF signal is generated by the signal generator and amplified by the pre-amplifier, transferring to each T/R channel through the $1:768$ power distribution network. Output power signal in the working channel is coupled to the $1:768$ power combining network by the directional coupler and transfers to the ICU and the receiver. In receive state, the signal from the signal generator is divided by the $1:768$ network and coupled to each T/R channel. The amplified signal in the working channel transfers to the receiver through the $1:768$ network, preamplifier, and ICU. The phase and gain of all T/R channels are controlled by the beam-control system. The amplitude and phase of each channel could be measured rapidly by internal calibration. In ground test, we can also replace the signal generator, ICU, and receiver as a vector network analyzer.

Figure 3 exhibits the schematic diagram of the directional coupler of each T/R channel. The four ports of the coupler are connected to the T/R channel, antenna subarray, the internal calibration network, and matched load. We take the example of the transmit state. When the input signal is in port 1, $C = P_3/P_1$ is defined as the coupling coefficient, and $D = P_4/P_3$ is defined as directionality. If the input signal voltage from a T/R channel is defined as V_{in}, the output voltage V_{out} to the internal calibration network is as follows:

$$V_{out} = V_{coupling} + V_{error} = CV_{in} + CD\left(V_{in}e^{j\theta_A}\Gamma_A + V_{in}e^{j\theta_L}\Gamma_L\right), \tag{2}$$

where, Γ_A and Γ_L are the reflection coefficient of antenna and load, θ_A and θ_L are the phases of the reflected signals from antenna and load. $V_{out} = CV_{in}$ is the ideal coupling signal. We can get the coupling error V_{error} as follows:

$$\frac{V_{error}}{V_{coupling}} = D\left(e^{j\theta_A}\Gamma_A + e^{j\theta_L}\Gamma_L\right). \tag{3}$$

In GF-3 SAR antenna system, the typical values are: $C = -25$ dB, $D = -20$ dB, $\Gamma_A = 0.33$ (VSMR = 2), and $\Gamma_L = 0.2$ (VSMR = 1.5). Thus

$$\frac{V_{error}}{V_{coupling}} = 0.033e^{j\theta_A} + 0.02e^{j\theta_L}. \tag{4}$$

For the worst case, the maximum amplitude error is 0.47 dB and the maximum phase error is 3.0° but not reached at the same time. This error level is acceptable for antenna pattern calculating, indicating that the excitation coefficient of each T/R channel could be measured by the internal calibration method with high accuracy with the application of directional couplers.

3.3. Internal Calibration Measurement Steps.

To carry out the internal calibration method, first, the basic data of the antenna should be obtained in a planar near-field measurement system, and second, we should get the amplitude and phase of all T/R channels for each antenna beam to calculate the pattern. The steps are the following:

(1) Put the phased array antenna in the microwave dark room and then, adjust the parallelism of the scanning probe and the antenna to the best. The parallelism between the GF-3 SAR antenna and the probe is better than 2 mm.

(2) Measure the patterns of all antenna subarrays, which are defined as $f_{mn}(u,v)$. It is described in detail in section 3.4.

(3) Set all the T/R channels to zero-state and calibrate the amplitude and phase of each T/R channel in the near-field to ensure that all the channels are excited by the same phase and amplitude. Be careful to control the temperature field distribution of the SAR antenna panel.

(4) Set the antenna in calibrated boresight beam state. By the near-field measurement, get the excitation coefficient of each T/R channel as A_{mn}. By internal calibration network, obtain the excitation coefficient of each T/R channel as $D0_{mn}$.

(5) Set the antenna in the state of the beam to be tested and get the excitation coefficient of each T/R channel by internal calibration as $D1_{mn}$.

(6) The excitation coefficient of the beam to be tested is $a_{mn} = A_{mn} + D1_{mn} - D0_{mn}$. Then, calculate the antenna pattern from the antenna model in formula (1).

Parameters $f_{mn}(u,v)$, A_{mn}, and $D0_{mn}$ are referred to as antenna base data and will be measured only once. For different beams in an on-ground test or in-orbit test, we just need to get the data $D1_{mn}$ in real-time and calculate the pattern. The measurement time of the internal calibration method is less than 1 minute.

The accuracy of $D1_{mn}$ has been guaranteed by the design of internal calibration RF loops. All the T/R channels are measured by the same signal generator and receiver, so the system test errors are canceled. High accuracy of the antenna model is achieved by precise on-ground measurements of antenna base data.

3.4. Antenna Subarray Antenna.

The radiating antenna panel consists of 768 dual-polarized subarrays (24 in azimuth and 32 in elevation). The pattern of embedded subarrays is different from subarrays in free space. Figure 4 displays the diagram of the waveguide slot antenna in the elevation direction. Each antenna subarray is composed of a vertically polarized broad wall slotted waveguide antenna and a horizontally polarized narrow wall slotted waveguide antenna, so the two independent antennas are physically isolated, reducing the cross-polarization level.

The antenna subarray patterns are measured by the near-field method: when the T/R channel corresponding to the subarray to be tested is working, we sample the near-field of the subarray and calculate the pattern. This measurement is time-consuming but it is necessary for improving the precision of the antenna model. In the antenna pattern model, mutual coupling between antenna subarrays is ignored, thus internal calibration method is not appropriate in tight coupling antenna arrays.

Figures 5(a) and 5(b) display the elevation pattern of H-polarization and V-polarization antenna subarrays at different positions. Patterns of H(V)17-H(V)32 are symmetric with H(V)16-H(V)1. The boundary conditions of the embedded subarrays in the middle of the antenna are the same, indicating the possibility of testing simplicity. For H-polarization, patterns of H3-H16 are almost identical, and the subarray patterns could be simplified into five types: H1, H2, H_{center}, H31, and H32. For V-polarization, patterns of V4-V16 are almost identical, and the subarray patterns could be simplified into seven types: V1, V2, V3, V_{center}, V30, V31, and V32. Thus, we can only measure 5/32 of H-polarization
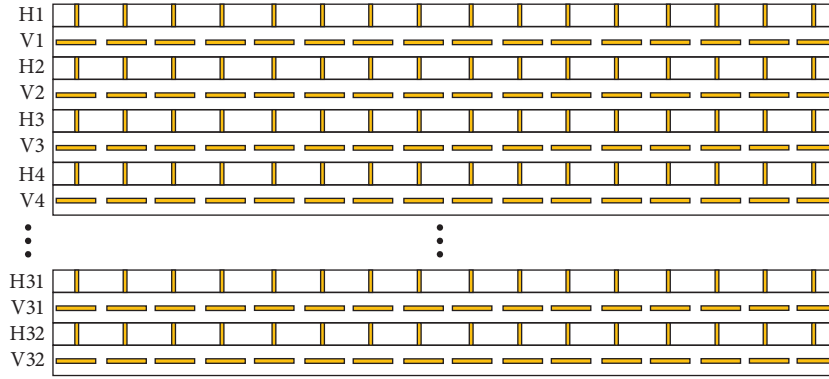
FIGURE 4: The diagram of the waveguide slot antenna in the elevation direction.
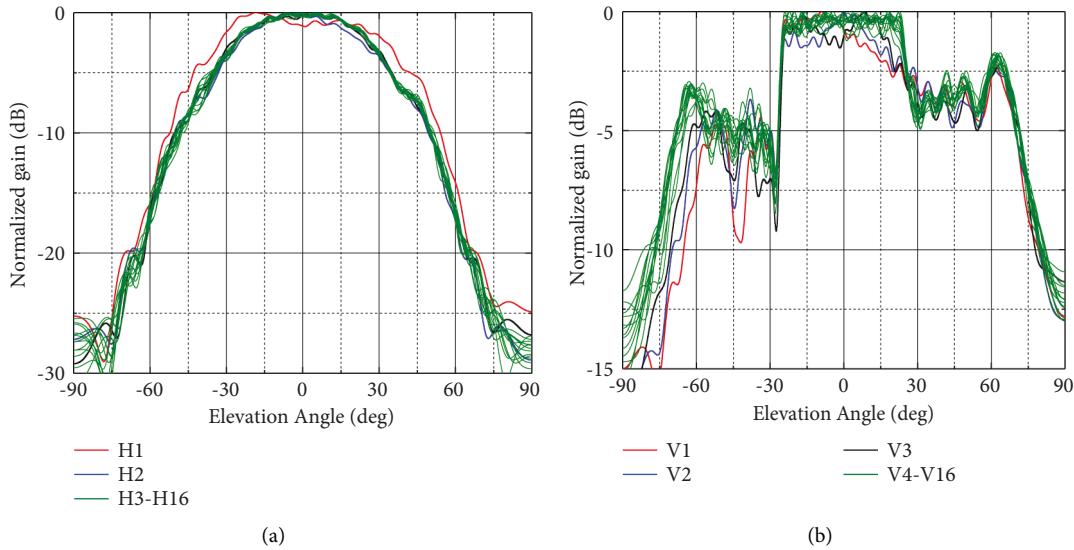

(a)

(b)

FIGURE 5: (a) Elevation pattern of H-polarization waveguide slot antenna. (b) Elevation pattern of V-polarization waveguide slot antenna.

subarrays and 7/32 of V-polarization subarrays to reduce the workload.

4. Results

To verify the performance of the internal calibration method, we compare the antenna pattern results of the internal calibration method (ICM) with the near-field method (NFM).

4.1. Internal Calibration Errors. In the GF-3 SAR antenna system, the phase shifter and attenuator in the T/R channel are 6 bits, meaning that the minimum phase step is 5.625°, and the minimum receive amplitude step is 0.5 dB. The internal calibration errors for the S1 beam (4 times broadened) are shown in Figure 6, which is the difference between the internal calibration value compared with the ideal phase and amplitude value. These errors are the sum of phase shifter/attenuator error and internal calibration network error. The root mean square (RMS) of amplitude errors and phase errors are 0.3 dB and 2.3° respectively, which are negligible in large phase array antenna.

4.2. Typical Elevation Pattern. First, we compare the elevation pattern results of ICM and NFM, which are shown in Figure 7. We take the boresight beam, 1.8 times broadened beam and 3.4 times broadened beam for example. These beams are measured in receive state with both the phase and amplitude of every T/R channel controlled. For the boresight beam, all lobes between −60° and +60° are well aligned. The main lobe difference between the two patterns is less than 0.1 dB, and the side-lobe difference is less than 0.5 dB between −40° and +40°. For the broadened beams, the main lobes of the two patterns are well aligned, and the deviation within the 3 dB main lobe is smaller than 0.1 dB, indicating that the elevation pattern results of the internal calibration method are in good agreement with the near-field method.

4.3. Typical Azimuth Pattern. Figure 8 shows the azimuth pattern comparison of ICM to NFM. We take the boresight beam and 1.7 times broadened beam for example. The two beams are measured in transmit state with only the phase of each T/R channel controlled. For the boresight beam, the
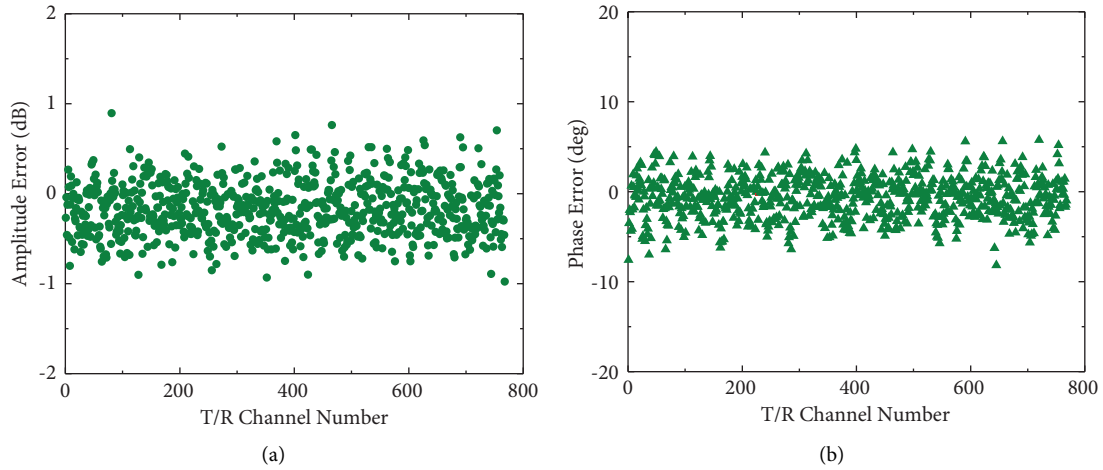
(a)

(b)

FIGURE 6: Internal calibration errors of 768 T/R channels for S1 beam. (a) Amplitude errors, the RMS value is 0.3 dB. (b) Phase errors, the RMS value is 2.3°.
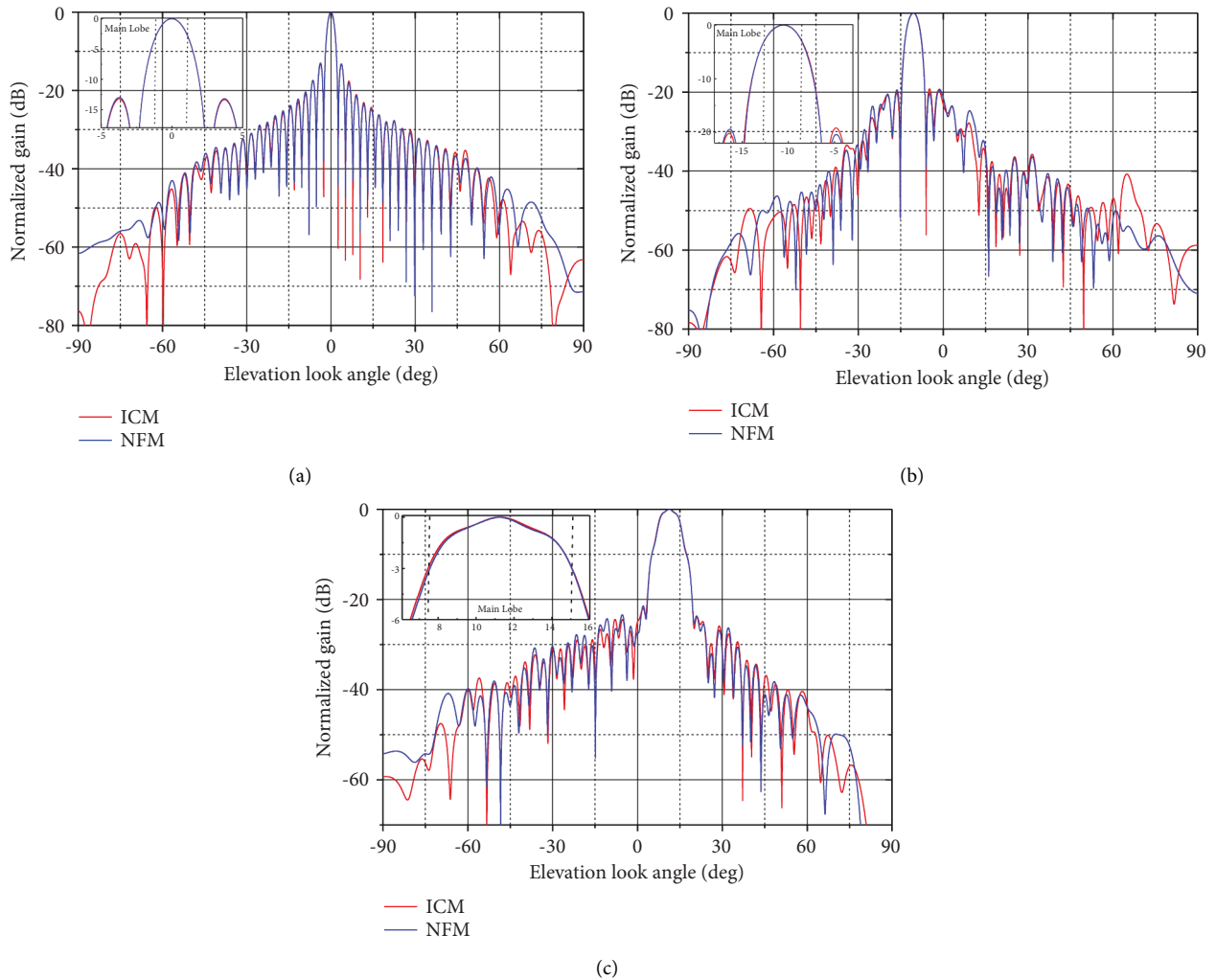

ICM
NFM

(a)

ICM
NFM

(b)

ICM
NFM

(c)

FIGURE 7: Elevation pattern comparison of the internal calibration method (ICM) to the near-field method (NFM). (a) Boresight beam. (b) Beam scanning and broadening 1.8 times. (c) Beam scanning and broadening 3.4 times. The inserts are the zoomed plots of the main lobe.
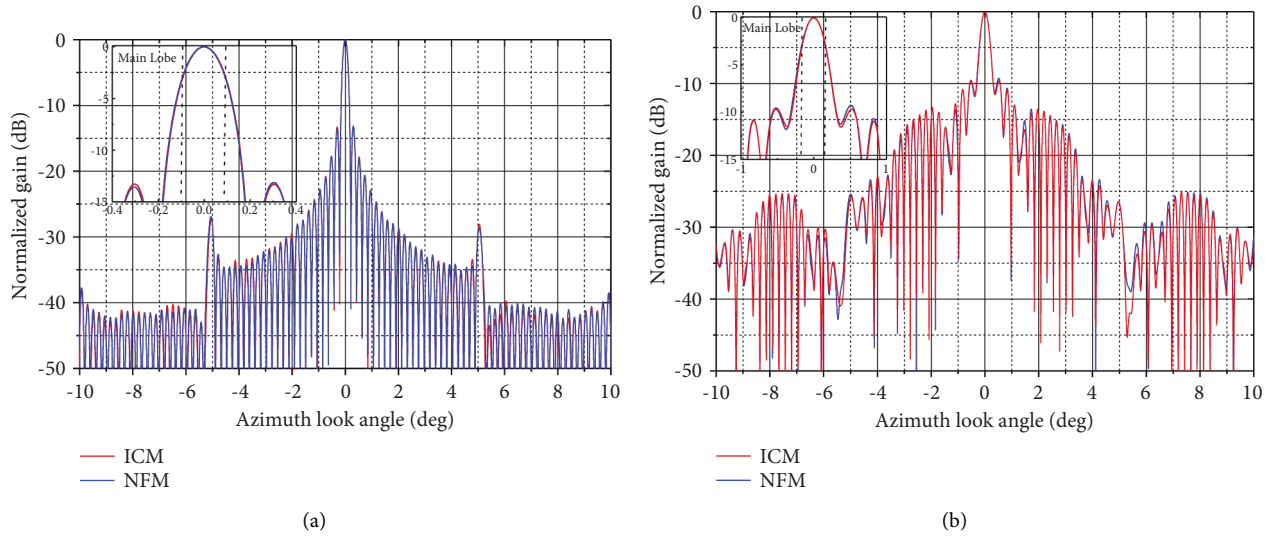
(a)

(b)

FIGURE 8: Azimuth pattern comparison of the internal calibration method (ICM) to the near-field method (NFM). (a) Boresight beam; (b) Beam broadening 1.7 times. The inserts are the zoomed plots of the main lobe.
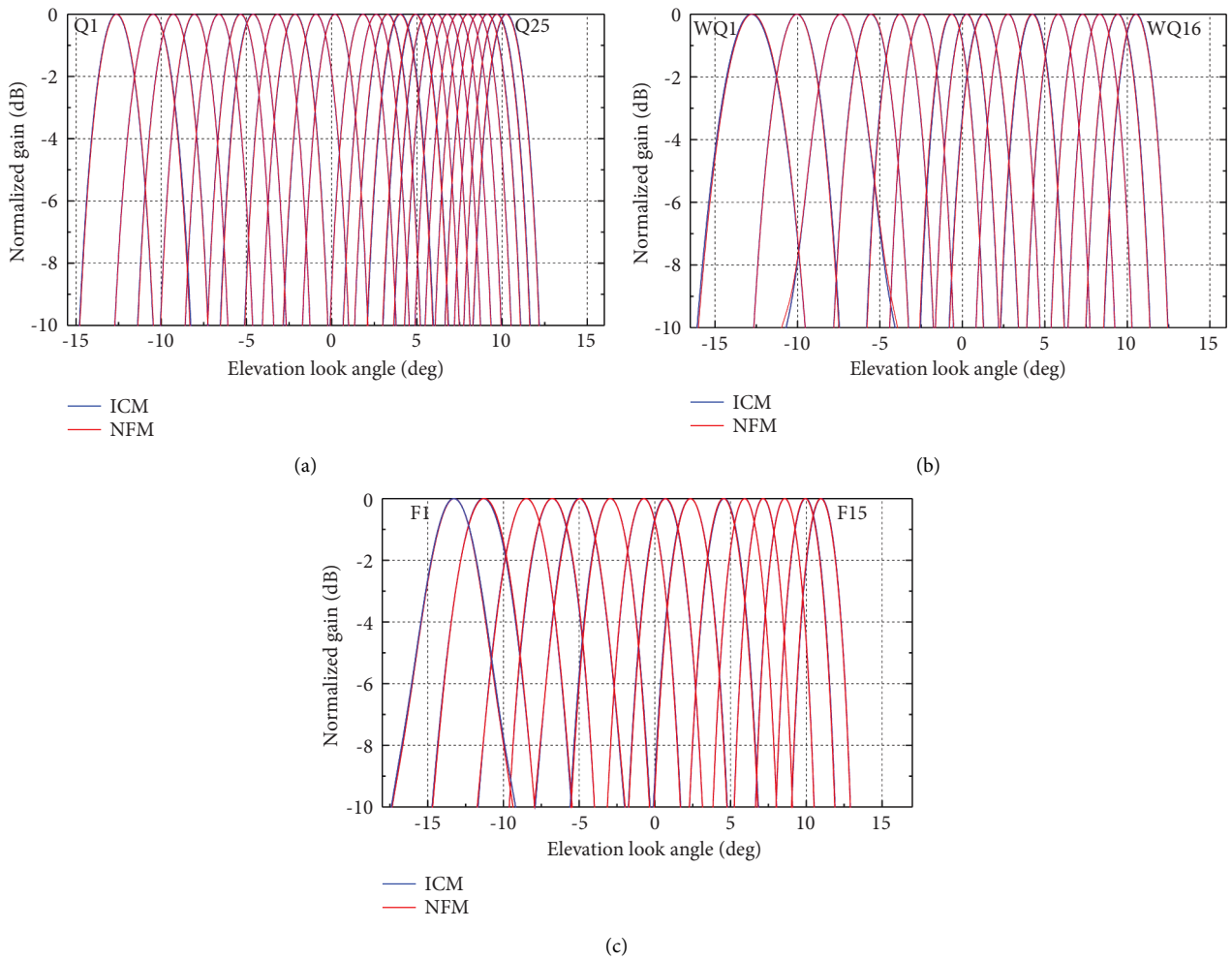

(a)

(b)

(c)

FIGURE 9: Elevation pattern comparison of the internal calibration method (ICM) to the near-field method (NFM) for typical observing modes. (a) Quad-pol stripmap mode (Q mode). (b) Wide quad-pol stripmap mode (WQ mode). (c) Fine stripmap mode (F mode).
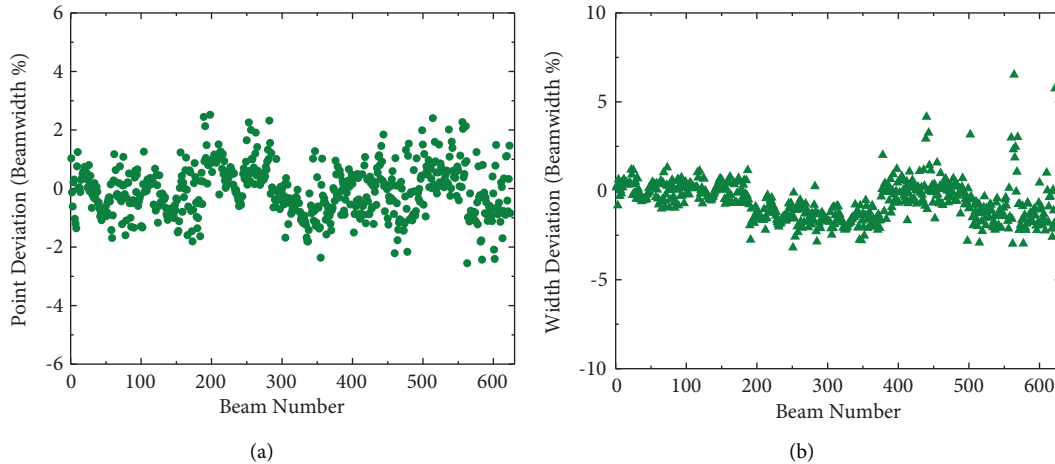
(a)

(b)

FIGURE 10: Beam deviation statistics. (a) Beam point deviation. (b) Beamwidth deviation.

3 dB beamwidth is 0.226°, and all lobes between -40° and +40° are well aligned, including grating lobes. The main lobe difference between the two patterns is less than 0.15 dB. For the broadened beam, all lobes between −40° and +40°are well aligned, and the deviation within the 3 dB main lobe is smaller than 0.15 dB, indicating that the azimuth pattern results of the internal calibration method are in good agreement with the near-field method.

4.4. Typical Observing Mode. GF-3 is a multipolarization SAR satellite, and the most typical observing mode is quad-polarization. We take quad-pol stripmap mode (Q), wide quad-pol stripmap mode (WQ), and fine stripmap mode (F) as examples to compare the elevation pattern of ICM and NFM. The results are exhibited in Figure 9, showing a maximum of 0.15 dB deviation within the 3 dB main lobe corresponding to the imaging area for all beams. The antenna pattern results of the two methods are good and consistent within the full elevation range.

4.5. Beam Deviation Statistics. In summary, we compare the results of the two methods for more than 600 beams, covering transmit and receive states and H and V polarizations. The elevation look angle is from −20°to +20° and the beamwidth is from nonbroadened to 4 times broadened. The beam point and beamwidth deviations are shown in Figure 10. The beam point deviations are smaller than 3% beamwidth, and the beamwidth deviations are less than 6% beamwidth (less than 4% for all beams except 2 beams). The beam deviation statistics indicate that the pattern results of the two methods are highly consistent in most cases, and we can utilize the internal calibration method to replace the near-field method for fast SAR antenna pattern measurement.

5. Conclusion

GF-3 is the first C-band multipolarization SAR satellite in China. In order to meet the multiuser requirements, twelve

observing modes were proposed and lots of antenna beams are needed to test for SAR image correction. The traditional method for antenna pattern measurement is the near-field method, but it is time-consuming, costly, and could not be carried out when the satellite is in orbit. To overcome the disadvantage of the near-field method, the internal calibration method is utilized for measuring the SAR antenna pattern.

This paper focuses on the internal calibration method, including its principle, operation steps, and results compared to the near-field method. Many efforts must be made to obtain the antenna base data such as the antenna subarray patterns, in order to establish an accurate SAR antenna model. The antenna pattern is calculated with the real-time internal calibration data and the model. The results of the internal calibration methods and the near-field method are highly consistent, indicating high accuracy and high efficiency of the new method.

The internal calibration method can be utilized in both ground tests and in-orbit tests. Furthermore, this technique is applicable for inflight SAR antenna measurement of other advanced sensor systems featuring phased array antennas.

Data Availability

The data used to support the findings of this study are available from the corresponding author upon request.

Conflicts of Interest

The authors declare that they have no conflicts of interest.

References

[1] Q. Zhang, "System design and key technologies of GF-3 satellite," *Acta Geodaetica et Cartographica Sinica*, vol. 46, pp. 269–277, 2017.

[2] Q. Zhang and Y. Liu, "Overview of Chinese first C band multipolarization SAR satellite GF-3," *Aerospace China*, vol. 18, pp. 22–31, 2017.

[3] J. Sun, W. Yu, and Y. Deng, "The SAR payload design and performance for the GF-3 mission," *Sensors*, vol. 17, no. 10, p. 2419, 2017.

[4] J. Mi, H. Sun, G. Song, Y. Xing, and X. Zhao, "Realization of low cross-polarization level for GF-3 SAR antenna," *International Journal of Antennas and Propagation*, vol. 2022, Article ID 9260843, 8 pages, 2022.

[5] M. Bachmann, M. Schwerdt, and B. Brautigam, "TerraSAR-X antenna calibration and monitoring based on a precise antenna model," *IEEE Transactions on Geoscience and Remote Sensing*, vol. 48, no. 2, pp. 690–701, 2010.

[6] Y. Gong, R. Wang, and P. Wang, "Improved phase-encoding calibration for active phased-array antennas of SAR," *IEEE Geoscience and Remote Sensing Letters*, vol. 13, no. 6, pp. 767–771, 2016.

[7] G. He, X. Gao, and R. Zhang, "Impact analysis and calibration methods of excitation errors for phased array antennas," *IEEE Access*, vol. 9, pp. 59010–59026, 2021.

[8] J. Uher, C. Grenier, and G. Lefebvre, "RADARSAT-2 SAR antenna," *Canadian Journal of Remote Sensing*, vol. 30, no. 3, pp. 287–294, 2004.

[9] R. J. Mailloux, *Phased Array Antenna Handbook*, Artech House, Norwood, MA, USA, 2005.

[10] J. Reimann and M. Schwerdt, "Technique for concurrent internal calibration during data acquisition for SAR systems," *Remote Sensing*, vol. 12, no. 11, pp. 1773–1781, 2020.

[11] G. Kuznetsov, V. Temchenko, M. Miloserdov, and D. Voskresenskiy, "Modifications of active phased antenna arrays near-field diagnosis method based on compressive sensing," *International Journal of Microwave and Wireless Technologies*, vol. 11, no. 7, pp. 568–576, 2019.

[12] T. Qiu, Y. Wang, J. Hong, K. Xing, S. Du, and J. Mu, "An in-orbit measurement method for elevation antenna pattern of MEO synthetic aperture radar based on nano calibration satellite," *Remote Sensing*, vol. 14, no. 3, p. 741, 2022.

[13] A. Bojarski, M. Bachmann, J. Böer et al., "TanDEM-X long-term system performance after 10 Years of operation," *Ieee Journal of Selected Topics in Applied Earth Observations and Remote Sensing*, vol. 14, pp. 2522–2534, 2021.

[14] https://sentinel.esa.int/web/sentinel/technical-guides/sentinel-1-sar/cal-val-activities/calibration/internal.